RESEARCH ARTICLE SUMMARY

HIV-1 VACCINES

Diversion of HIV-1 vaccine–induced immunity by gp41-microbiota cross-reactive antibodies

Wilton B. Williams,* Hua-Xin Liao, M. Anthony Moody, Thomas B. Kepler, S. Munir Alam, Feng Gao, Kevin Wiehe, Ashley M. Trama, Kathryn Jones, Ruijun Zhang, Hongshuo Song, Dawn J. Marshall, John F. Whitesides, Kaitlin Sawatzki, Axin Hua, Pinghuang Liu, Matthew Z. Tay, Kelly E. Seaton, Xiaoying Shen, Andrew Foulger, Krissey E. Lloyd, Robert Parks, Justin Pollara, Guido Ferrari, Jae-Sung Yu, Nathan Vandergrift, David C. Montefiori, Magdalena E. Sobieszczyk, Scott Hammer, Shelly Karuna, Peter Gilbert, Doug Grove, Nicole Grunenberg, M. Juliana McElrath, John R. Mascola, Richard A. Koup, Lawrence Corey, Gary J. Nabel,† Cecilia Morgan, Gavin Churchyard, Janine Maenza, Michael Keefer, Barney S. Graham, Lindsey R. Baden, Georgia D. Tomaras, Barton F. Haynes*

INTRODUCTION: Inducing protective antibodies is a key goal in HIV-1 vaccine development. In acute HIV-1 infection, the dominant initial plasma antibody response is to the gp41 subunit of the envelope (Env) glycoprotein of the virus. These antibodies derive from polyreactive B cells that cross-react with Env and intestinal microbiota (IM) and are unable to neutralize HIV-1. However, whether a similar gp41-IM cross-reactive antibody response would occur in the setting of HIV-1 Env vaccination is unknown.

RATIONALE: We studied antibody responses in individuals who received a DNA prime vaccine, with a recombinant adenovirus serotype 5 (rAd5) boost (DNA prime–rAd5 boost), a vaccine that included HIV-1 *gag*, *pol*, and *nef* genes, as well as a trivalent mixture of clade A, B, and C *env* gp140 genes containing both gp120 and gp41 components. This vaccine showed no efficacy. Thus, study of these vaccinees provided an opportunity to determine whether the Env-reactive antibody response in the setting of Env vaccination was dominated by gp41-reactive antibodies derived from Env-IM cross-reactive B cells.
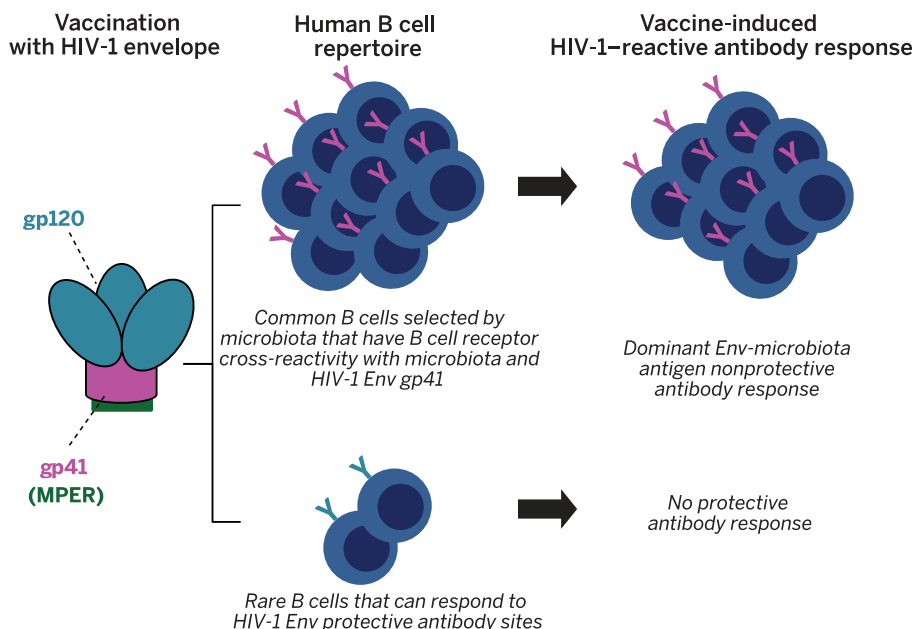
RESULTS: We found that vaccine-induced antibodies to HIV-1 Env dominantly focused on gp41 compared with gp120 by both serologic analysis and by vaccine-Env memory B cells

sorted by flow cytometry (see the figure). Remarkably, the majority of HIV-1 Env-reactive memory B cells induced by the vaccine produced gp41-reactive antibodies, and the majority of gp41-targeted antibodies used restricted immunoglobulin heavy chain variable genes. Functionally, none of the gp41-reactive antibodies could neutralize HIV, and the majority could not mediate antibody-dependent cellular cytotoxicity. Most of the vaccine-induced gp41-reactive antibodies cross-reacted with host and IM antigens. Two of the candidate gp41-intestinal cross-reactive antigens were bacterial RNA polymerase and pyruvate-flavodoxin oxidoreductase, which shared sequence similarities with the heptad repeat 1 region of HIV gp41. Next-generation sequencing of vaccinee B cells demonstrated a prevaccination antibody that was reactive to both IM and the vaccine–Env gp140, which demonstrated the presence of a preexisting pool of gp41-IM cross-reactive B cells from which the vaccine gp41-reactive antibody response was derived.

CONCLUSION: In this study, we found that the DNA prime–rAd5 boost HIV-1 vaccine induced a gp41-reactive antibody response that was mainly non-neutralizing and derived from an IM-gp41 cross-reactive B cell pool. These findings have important implications for HIV-1 vaccine design. Because IM antigens shape the B cell repertoire from birth, our data raise the hypothesis that neonatal immunization with HIV-1 envelope may be able to imprint the B cell repertoire to respond to envelope antigenic sites that may otherwise be subdominant or disfavored, such as Env broadly neutralizing antibody epitopes. Our data also suggest that deleting or modifying amino acids in the gp41 heptad repeat 1 region of Env-containing vaccine immunogens may avoid IM-gp41 cross-reactivity. Thus, an obstacle that may need to be overcome for development of a successful HIV vaccine is diversion of potentially protective HIV-1 antibody responses by preexisting envelope-IM cross-reactive pools of B cells. ∎

Vaccination with HIV-1 envelope • Human B cell repertoire • Vaccine-induced HIV-1–reactive antibody response

gp120
gp41 (MPER)

Common B cells selected by microbiota that have B cell receptor cross-reactivity with microbiota and HIV-1 Env gp41

Dominant Env-microbiota antigen nonprotective antibody response

Rare B cells that can respond to HIV-1 Env protective antibody sites

No protective antibody response

Diversion of HIV-1 vaccine–induced immunity by Env gp41–microbiota cross-reactive antibodies. Immunization of humans with a vaccine containing HIV-1 Env gp120 and gp41 components, including the membrane-proximal external region (MPER) of Env, induced a dominant B cell response primarily from a preexisting pool of gp41-IM cross-reactive B cells. This response diverted the vaccine-stimulated antibody response away from smaller subdominant B cell pools capable of reacting with potentially protective epitopes on HIV-1 Env.

HIV-1 VACCINES

Diversion of HIV-1 vaccine–induced immunity by gp41-microbiota cross-reactive antibodies

Wilton B. Williams,[1]* Hua-Xin Liao,[1] M. Anthony Moody,[1] Thomas B. Kepler,[2] S. Munir Alam,[1] Feng Gao,[1] Kevin Wiehe,[1] Ashley M. Trama,[1] Kathryn Jones,[1] Ruijun Zhang,[1] Hongshuo Song,[1] Dawn J. Marshall,[1] John F. Whitesides,[1] Kaitlin Sawatzki,[2] Axin Hua,[2] Pinghuang Liu,[1] Matthew Z. Tay,[1] Kelly E. Seaton,[1] Xiaoying Shen,[1] Andrew Foulger,[1] Krissey E. Lloyd,[1] Robert Parks,[1] Justin Pollara,[1] Guido Ferrari,[1] Jae-Sung Yu,[1] Nathan Vandergrift,[1] David C. Montefiori,[1] Magdalena E. Sobieszczyk,[3] Scott Hammer,[3] Shelly Karuna,[4] Peter Gilbert,[5] Doug Grove,[5] Nicole Grunenberg,[4] M. Juliana McElrath,[4] John R. Mascola,[6] Richard A. Koup,[6] Lawrence Corey,[4] Gary J. Nabel,[6]† Cecilia Morgan,[5] Gavin Churchyard,[7] Janine Maenza,[4] Michael Keefer,[8] Barney S. Graham,[6] Lindsey R. Baden,[9] Georgia D. Tomaras,[1] Barton F. Haynes[1]*

An HIV-1 DNA prime vaccine, with a recombinant adenovirus type 5 (rAd5) boost, failed to protect from HIV-1 acquisition. We studied the nature of the vaccine-induced antibody (Ab) response to HIV-1 envelope (Env). HIV-1–reactive plasma Ab titers were higher to Env gp41 than to gp120, and repertoire analysis demonstrated that 93% of HIV-1–reactive Abs from memory B cells responded to Env gp41. Vaccine-induced gp41-reactive monoclonal antibodies were non-neutralizing and frequently polyreactive with host and environmental antigens, including intestinal microbiota (IM). Next-generation sequencing of an immunoglobulin heavy chain variable region repertoire before vaccination revealed an Env-IM cross-reactive Ab that was clonally related to a subsequent vaccine-induced gp41-reactive Ab. Thus, HIV-1 Env DNA-rAd5 vaccine induced a dominant IM-polyreactive, non-neutralizing gp41-reactive Ab repertoire response that was associated with no vaccine efficacy.

I n acute HIV-1 infection, the dominant initial plasma antibody (Ab) response is to the gp41 subunit of the envelope (Env) glycoprotein of the virus (1). This Ab response derives from polyreactive B cells that cross-react with Env and intestinal microbiota (IM) (2, 3). However, it is unknown if a similar gp41-reactive Ab response would occur in the setting of HIV-1 Env vaccination. A DNA prime vaccine, with a recombinant adenovirus serotype 5 (rAd5) boost (DNA prime–rAd5 boost), a vaccine that included HIV *gag*, *pol*, and *nef* genes—as well as a trivalent mixture of clade A, B, and C *env* gp140 genes containing both gp120 and gp41 components—was studied in the HIV Vaccine Trials Network (HVTN) [phase Ib (HVTN 082), phase II (HVTN 204), and phase IIb (HVTN 505) efficacy trial] and other clinical trials [phase I/II (RV172) and phase I (V001)] (4–7). This vaccine was the first vaccine containing the ectodomain of the Env gp41 component, covalently linked to gp120, to be tested in an efficacy trial and was designed to generate primarily CD8 T cell responses, although this vaccine generated Env Ab responses as well (8–10). However, the phase IIb HVTN 505 efficacy trial showed no vaccine efficacy (11). Thus, these vaccine trials containing Env gp41 provided an opportunity to determine whether the Env Ab response in the setting of Env vaccination was dominated by gp41-reactive Abs derived from Env-IM cross-reactive B cells.

Isolation of Env-reactive memory B cells and vaccinee plasma serologies

We found that the DNA prime–rAd5 boost Ab response to HIV-1 Env was dominantly focused on gp41 compared with gp120. This specificity was demonstrated by both serologic analysis and vaccine-Env flow cytometry–sorted memory B cells. Plasma immunoglobulin G (IgG)–binding assays were performed on plasma of a random sample of 40 phase IIb (efficacy trial) vaccine recipients who were HIV-1 negative at the final, month 24, visit (11) (Fig. 1A), as well as plasma of eight HIV-1 uninfected phase Ib and II DNA prime–rAd5 boost trial participants with high titers of plasma-binding Abs to recombinant (r) gp140 vaccine–Envs and/or neutralization of clade C HIV-1 isolate MW965 (Fig. 1B). Plasma-binding gp41-reactive Ab titers were ≥10 times as much as gp120-reactive Ab titers, including Ab reactivity with vaccine-gp120s [($P < 0.0001$) (Fig. 1A), $P < 0.01$ (Fig. 1B); Wilcoxon signed rank test]. Thus, the nonprotective DNA prime–rAd5 boost gp140 vaccine induced a dominant HIV-1 Env gp41 response in plasma Abs.

Next, we performed single memory B cell sorting by flow cytometry using peripheral blood B cells from phase Ib and phase II DNA prime, rAd5-boost, trial participants. Vaccine-Env gp140 and V1V2 subunits—as well as a consensus group M gp140 Env (termed CON-S) (12)—were used as fluorophore-labeled recombinant proteins to identify Env-specific memory B cells present in peripheral blood mononuclear cells (PBMCs) of vaccinees 4 weeks after final vaccination (fig. S1 and table S1). We studied eight phase Ib and phase II DNA prime, rAd5-boost, trial participants; from these eight vaccinees, we isolated 221 HIV-1 Env-reactive Abs (Fig. 1C and table S2). Of the 221 HIV-1 Env-reactive Abs, there were 131 unique V_HDJ_H rearrangements (table S3). Remarkably, 205 out of 221 (205/221) (93%) of the HIV-1 Env-reactive Abs and 115/131 (88%) of the unique heavy chain sequences induced by the vaccine were gp41-reactive, with only 7% (16/221) gp120-reactive (tables S3 to S6). We used Ab gene transient transfections to perform enzyme-linked immunosorbent assays (ELISAs) to determine gp41 versus gp120 reactivity (13). Of the Env-reactive Abs, 16/16 (100%) gp120-reactive and 195/205 (95%) gp41-reactive Abs bound vaccine-rgp140 proteins. The 10 gp41-reactive Abs that bound only heterologous recombinant Env proteins likely recognized gp41 epitopes expressed on the vaccine protein generated by DNA or rAd5 that were not expressed on the rgp140 proteins.

We asked if there were indeed fewer gp120-reactive memory B cells from gp140-vaccinated individuals who received the DNA prime–rAd5 boost vaccine compared with gp140-reactive memory B cells. In three phase II trial vaccinee memory B cell samples, we found that Vaccine Research Center (VRC)–A gp120 bound to 0.37% of memory B cells compared with 0.55% of memory B cells by VRC-A gp140 ($P < 0.001$; Cochran-Mantel-Haenszel test) (fig. S2). Of the gp41-reactive and gp120-reactive Abs isolated from the eight phase Ib and II vaccinees, 112/221 (52%) were sorted using the group M consensus CON-S gp140 as a fluorophore-labeled hook. CON-S rgp120 bound to 0.05% memory B cells in comparison with 0.28% by CON-S gp140 ($P < 0.001$, Cochran-Mantel-Haenszel test). Of total HIV-1 Env-reactive memory B cells, CON-S gp120 bound to 13% (38/292), whereas 87% of Env-reactive memory B cells (254/292) reacted with CON-S gp140 (fig. S2). Therefore, the dearth of isolated gp120-reactive

[1]Duke Human Vaccine Institute, Duke University School of Medicine, Durham, NC, USA. [2]Department of Microbiology, Boston University School of Medicine, Boston, MA, USA. [3]Department of Medicine, Columbia University Medical Center, New York, NY, USA. [4]Vaccine and Infectious Disease Division, Fred Hutchinson Cancer Research Center, Seattle, WA, USA. [5]The Statistical Center for HIV/AIDS Research and Prevention (SCHARP), Fred Hutchinson Cancer Research Center, Seattle, WA, USA. [6]Vaccine Research Center, National Institute of Allergy and Infectious Diseases, National Institutes of Health, Bethesda, MD, USA. [7]The Aurum Institute, Johannesburg, South Africa. [8]University of Rochester School of Medicine, Rochester, NY, USA. [9]Brigham and Women's Hospital, Boston, MA, USA.
*Corresponding author. E-mail: barton.haynes@duke.edu (B.F.H.); wilton.williams@duke.edu (W.B.W.) †Present address: Sanofi, 640 Memorial Drive, Cambridge, MA 02139, USA.

Abs was mirrored by low frequencies of gp120-memory B cells in the blood of vaccinees.

For comparison, we have previously studied an Env gp120-only immunization trial in humans and demonstrated that at peak immunization the frequency of memory B cells ranged as high as 0.73% gp120-reactive B cells (mean 0.23 ± 0.1%) (*14*). In a rhesus macaque immunization study with gp120 alone, the frequency of memory B cells that were gp120-reactive was 3% (*15*). Thus, in the setting of gp120-only immunizations in humans and rhesus macaques, the memory B cell response to gp120 is robust.

Heavy chain gene restriction for HIV-1 gp41-reactive memory B cell Abs

We analyzed the variable heavy chain gene families used by HIV-1–reactive Abs induced by the DNA prime–rAd5 boost gp140 vaccine. Gp41-reactive Abs had a mean heavy chain nucleotide mutation frequency of 2.5% (fig. S3) and a median heavy chain complementarity-determining region 3 (HCDR3) length of 14 amino acids (fig. S4). Remarkably, of 137 total IGHV1-using Abs, 125 (91% of IGHV1-using Abs, 57% of total 221 HIV-1–reactive Abs) used a single V_H segment, IGHV1-69 (table S7). To rule out IGHV1-69 predominance as a result of polymerase chain reaction (PCR) primer bias, we examined the heavy chain gene usage of non–HIV-1–reactive Abs isolated from all eight vaccinees; only 12% (18/145) of non–HIV-1–reactive Abs used IGHV1-69 ($P < 0.0001$, Fisher's exact test). The 125 IGHV1-69–using HIV-1–reactive Abs all reacted with gp41, and 94 (75%) were found to be naturally paired with a kappa light chain and 31 (25%) with a lambda light chain. IGκV3-20 (48%, 60/94) and

IGλ2-14 (29%, 9/31) were the light chains preferentially paired with the IGHV1-69–using gp41-reactive Abs (table S8). Of gp41-reactive Abs, 66% (136 of 205 Abs) used the *IGHV1* gene family; 61% (125 of 205 gp41-reactive Abs) specifically used the *IGHV1-69* gene segment (table S9), compared with HIV-1–uninfected individuals, in whom 6% of the Ab repertoire used IGHV1-69 (*16*) ($P < 0.0001$, chi-square test). Of the gp41-reactive Abs, 132 paired with IGκV light chains (table S10), whereas 73 gp41-reactive Abs paired with IGλV light chains (table S11). Moreover, next-generation sequencing (NGS) of prevaccination heavy chain $V_H DJ_H$ rearrangements derived from RNA obtained from PBMCs of all eight vaccinees revealed ~5% IGHV1-69–using B cells before vaccination (tables S12). Thus, the frequency of IGHV1-69–using B cells was the same in healthy subjects as in prevaccination B cells but was dominantly used in the gp41 postvaccination repertoire, which indicated that the postvaccination gp41-reactive Ab IGHV1-69 usage induced by the DNA prime–rAd5 boost vaccine was not due to heavy chain gene primer bias but rather was selected by the vaccine.

There are 13 known allelic variants of *IGHV1-69* gene segment; 7 have a phenylalanine (F) at amino acid position 54 in the HCDR2 region (54F-HCDR2), and 6 have a leucine (L) (54L-HCDR2) (*17*). The ratio of 54F-HCDR2 to 54L-HCDR2 IGHV1-69 allelic variants in the global population is estimated to be 3:2 (*18*). Neutralizing influenza and HIV-1–reactive Abs use 54F-HCDR2 IGHV1-69 gene segments to bind hydrophobic pockets in the stems of hemagglutinin (HA) (*19*, *20*) and gp41 (*21*, *22*), respectively. Thus, we asked whether both allelic forms of the *IGHV1-69*

gene segment were equally represented in HIV-1 gp41-reactive Abs elicited by the DNA prime–rAd5 boost vaccine. Of 125 vaccine-induced IGHV1-69–using Abs, we found that 116 (93%) used 54L-HCDR2 variants, whereas only 9 (7%) used 54F-HCDR2 variants (Table 1 and table S5). NGS of prevaccination IGHV repertoire demonstrated that all eight phase Ib and II trial vaccinees encoded 54F- and 54L-HCDR2 variants of IGHV1-69 (table S12). Therefore, the expression of 54L-HCDR2 IGHV1-69 variants was not due to vaccinee inability to express 54F-HCDR2 variants. As a comparison, we asked what *IGHV1-69* gene allelic variants were used by gp41-reactive Abs in HIV-1 infection. Of 42 IGHV1-69–using gp41-reactive Abs from HIV-1–infected individuals (*23*), 41/42 (98%) used 54L-HCDR2 variants and 1/42 (2%) used a 54F-HCDR2 variant (Table 1). In contrast, of 64 non–HIV-1–reactive IGHV1-69–using Abs isolated from HIV-1 infected individuals (*2*, *3*, *23*), 18/64 (28%) used 54L-HCDR2 variants, whereas 46/64 (72%) used 54F-HCDR2 variants (Table 1). Finally, of 10 IGHV1-69–using influenza hemagglutinin Abs isolated from influenza vaccinees or acute influenza infection (*24*), 9 (90%) used 54F-HCDR2 variants and only 1 (10%) used a 54L-HCDR2 variant (Table 1). Thus, the DNA prime–rAd5 boost vaccine induced a dominant gp41-reactive Ab response that preferentially used 54L-HCDR2 IGHV1-69 allelic variants, similar to gp41-reactive Abs induced by HIV-1 infection ($P = 0.45$; Fisher's exact test) but different from influenza-induced IGHV1-69 Abs ($P < 0.0001$; Fisher's exact test) (Table 1 and table S5).

Because a subset of B-chronic lymphocytic leukemia (B-CLL) Abs uses IGHV1-69 and can
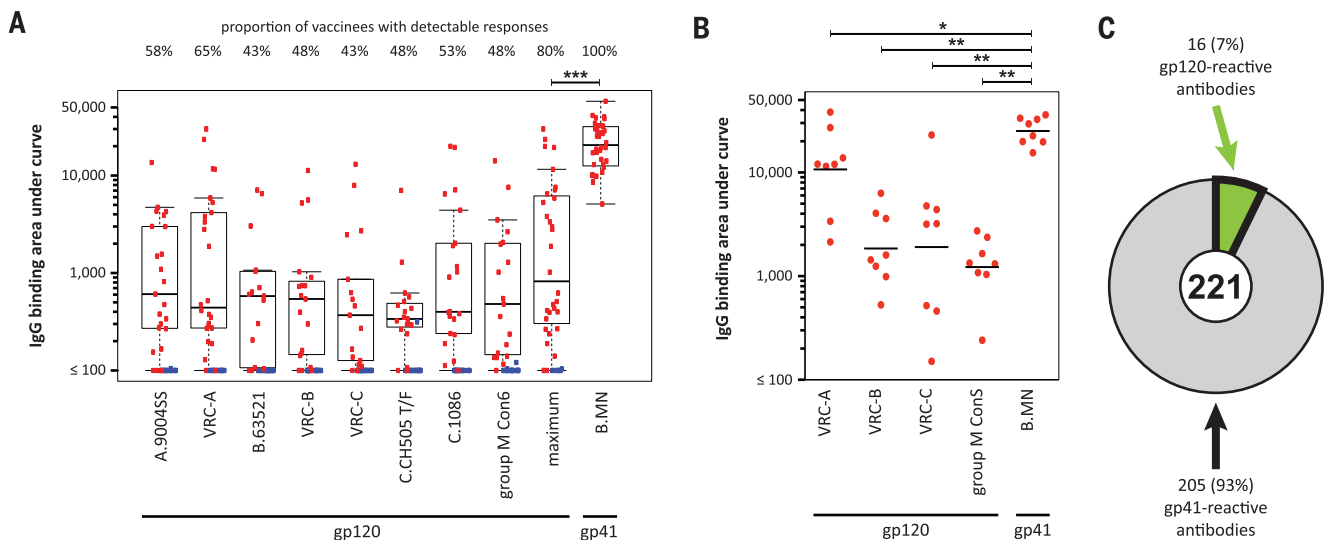
Fig. 1. Characteristics of HIV-1–reactive Abs induced by DNA prime–rAd5 boost vaccine. (**A**) Plasma Ab titers (AUC, area under the curve) to gp120 and gp41 proteins in a subset of 40 HVTN 505 vaccine recipients; red circles represent vaccine responders (percentages) to the antigens tested, and blue represent nonresponders. (**B**) Plasma binding Abs from eight HVTN 082 and 204 trial participants (vaccine responders) were screened for gp120 and gp41 reactivity by means of binding Ab multiplex assay (BAMA).

(**C**) HIV-1–reactive Abs were isolated from single memory B cells of the eight HVTN 082 and 204 trial participants and screened for binding gp120 and gp41 proteins by means of enzyme-linked immunosorbent assay (ELISA). Statistics: (A) ***$P < 0.0001$, Wilcoxon signed rank test, B.MN gp41 versus gp120 (maximum; which is the highest value of all gp120 Envs for each participant), *$P < 0.05$, McNemar's test; B.MN gp41 versus each gp120 (not shown); (B) *$P < 0.05$, **$P < 0.01$, Wilcoxon signed rank test [Graphpad Prism].

Table 1. Frequency of 54L- and 54F-HCDR2–bearing IGHV1-69–using Abs induced by HIV and influenza. Counts reflect number of unique Ab heavy chain sequences containing full V_HDJ_H rearrangements without stop codons. Cohorts: HIV-1 vaccination[1], 8 HVTN 204 and 082 trial participants; HIV-1 infection[2,3], 29 HIV-1–infected subjects (2, 3, 23); influenza[4], 13 influenza-infected or vaccinated subjects (24). Influenza Ab specificity as measured by reactivity with purified recombinant HA-enriched trivalent influenza vaccine (Fluzone)[5]. Statistics were produced by using Fisher's exact test and SAS.

Cohort	Ab reactivity	Total Abs	IGHV1-69 Abs	HCDR2-54L	HCDR2-54F	Statistics HCDR2-54L:54F
HIV-1 vaccination[1]	gp41	205	125/205 (61%)	116/125 (93%)	9/125 (7%)	$P < 0.45^{(1v2)}$
HIV-1 infection[2]	gp41	116	42/116 (36%)	41/42 (98%)	1/42 (2%)	
HIV-1 infection[3]	Non–HIV-1	971	64/971 (7%)	18/64 (28%)	46/64 (72%)	$P < 0.0001^{(1v3, 2v3)}$
Influenza infection or vaccination[4]	Hemagglutinin[5]	278	10/278 (4%)	1/10 (10%)	9/10 (90%)	$P < 0.0001^{(1v4, 2v4)}$; $P = 0.44^{(3v4)}$

cross-react with HIV-1 Env gp41 (23), we compared IGHV1-69 sequences of healthy control Abs (16), B-CLL Abs (23), and gp41-reactive Abs from phase Ib and II trials vaccine-recipients, for CLL archetypes previously described (25). We found that the frequency of CLL archetype matches in our vaccine-induced IGHV1-69–using Abs (1.6%) was no different from healthy control IGHV1-69 sequences (2.3%) but differed from CLL Abs (10.6%) (vaccine-induced gp41-reactive versus CLL Abs, $P = 0.002$; vaccine-induced gp41-reactive Abs versus healthy controls, NS; CLL versus healthy controls 1.7×10^{-5}, Fisher's exact test) (table S13). Thus, there is no evidence of selective derivation of vaccine-induced gp41-reactive IGHV1-69 Abs from the same pool of B cells that give rise to CLL Abs.

Functional properties of HIV-1–reactive mAbs

We chose 29 naturally paired heavy and light chain genes for recombinant Ab bulk expression and characterization; 17 gp41-reactive [representing 45 Abs within 17 vaccine-induced clonal lineages (table S14)] and 12 gp120-reactive [representing 12 clonal lineages (table S15)] monoclonal antibodies (mAbs). Gp41-reactive mAbs bound to rgp140 and/or gp41 proteins via ELISA and/or surface plasmon resonance (SPR) (table S16). For Abs that reacted strongly to vaccine Envs, the dissociation constants (K_d) for binding to gp41 MN recombinant protein of 5 gp41 mAbs ranged from ~1 to 71 nM, whereas binding to vaccine-Env VRC-A and heterologous group M consensus gp140 Envs ranged from ~1 to 23 nM (table S17). None of the gp41-reactive mAbs mediated neutralization using a panel of pseudotyped HIV-1 isolates: neutralization-resistant (tier 2) VRC-A (A.92RW020) and VRC-C (C.97ZA012), neutralization-sensitive (tier 1) B.HxB2 and B.BaL of VRC-B (B.HxB2/BaL-V3), and heterologous neutralization-sensitive (tier 1) B.MN (table S18). Only 1/17 (6%) gp41-reactive mAb captured infectious virions (B.NL4-3) (fig. S5A) or mediated Ab-dependent cell-mediated cytotoxicity (ADCC) (C.1086) (fig. S6). In contrast, one-third (4/12) of vaccine-induced gp120 mAbs neutralized at least 1 neutralization-sensitive HIV-1 isolate (table S19); all neutralizing gp120-reactive Abs targeted the third variable loop (V3) (mAbs

DH196, DH449, DH450, and DH452) and neutralized HIV-1 B.BaL and/or B.MN. Of the gp120-reactive mAbs, 2/12 (17%) captured infectious HIV-1 (fig. S5B), and 5/12 (42%) mediated ADCC (fig. S7).

Site of reactivity of vaccine-induced gp41 Abs

We previously reported that gp41-reactive Abs from HIV-1–infected patients are cross-reactive with the 37-kD subunit of bacterial *Escherichia coli* (*E. coli*) RNA polymerase (2). We identified a short region of sequence similarity between gp41 and bacterial RNA polymerase with a shared amino sequence of LRAI (amino acid numbering 556–559 in gp41 (PDB: 1AIK) and 43–46 in bacterial RNA polymerase) (PDB: 1BDF) (fig. S8A). A structural alignment of HIV-1 Env gp41 (26) and bacterial RNA polymerase (27) showed that the α-subunit helices at the RNA polymerase dimer interface were similar to a portion of the gp41 heptad repeat 1 (HR-1) and heptad repeat 2 (HR-2) helices with a 1.30 Å backbone atom root-mean-square deviation (fig. S8, B and C). This analysis raised the hypothesis that the VRC vaccine–induced gp41-reactive Abs may bind to the gp41 postfusion structure.

To determine binding sites for vaccine-induced gp41-reactive mAbs on vaccine VRC-A gp140 protein, we proteolytically cleaved the gp140 protein with trypsin and analyzed the cleavage products on SDS–polyacrylamide gel electrophoresis (SDS-PAGE) gels in Western blot analysis with three VRC-A gp140– and gp41-reactive (DH438, DH440, and DH432) and control mAbs and used liquid chromatography–mass spectrometry (LC-MS). We found a ~25-kD fragment of VRC-A gp140 that was blotted by the gp41, VRC-A gp140, and IM-reactive vaccine-induced mAbs and contained a peptide amino acid sequence (558–567, PDB: 1AIK) AIEAQQHLLQ that placed it in the HR-1 gp41 region overlapping with the LLRAIE gp41 sequence (amino acids 555–560, PDB: 1AIK) of HR-1 that was a putative cross-reactive region with the bacterial IM-protein, RNA polymerase (fig. S9). Thus, one region of VRC-A gp140 bound by HIV-1 gp41-reactive mAbs was in the gp41 HR-1 region.

In order to identify additional candidate proteins in IM that cross-reacted with gp41-reactive

Abs, SDS-PAGE gels were run with IM whole-cell lysates (WCLs) and analyzed in Western blots with VRC-A gp140, gp41, and IM-reactive IGHV1-69 mAbs DH438, DH440, and DH432. Analysis of IM sequences in bands reactive with one or more gp41-reactive mAbs revealed 19 candidate IM proteins by LC-MS (fig. S10, a and b). Alignment of candidate IM protein and gp41 sequences demonstrated one bacterial protein, pyruvate-flavodoxin oxidoreductase, that had a sequence similar to that of gp41 HR-1 amino acids 555–560 LLRAIE, with an amino acid sequence in pyruvate-flavodoxin oxidoreductase sequence amino acids 500–505 LLRGIK (fig. S10c). Thus, pyruvate-flavodoxin oxidoreductase is a second candidate protein that may cross-react with HIV-1 gp41-reactive Abs. That this sequence similarity between gp41 and pyruvate-flavodoxin oxidoreductase was the same as found for the tryptic fragment of DH438-bound VRC-A gp140 (fig. S9), as well as the sequence similarity found between gp41 and bacterial RNA polymerase (fig. S8), raised the hypothesis that gp41-reactive Abs induced by the VRC vaccine bind to an HR-1 sequence in the gp41 postfusion conformation. Indeed, vaccine-induced gp41-reactive mAbs DH438, DH432, and DH440 bound to linear peptides containing the LLRAIE HR-1 sequence (table S20), and 16/17 gp41-reactive mAbs bound a gp41 postfusion conformation recombinant protein (21) (table S16).

Polyreactivity of HIV-1–reactive mAbs

Binding to non–HIV-1 molecules was used to identify polyreactivity among these HIV-1–reactive Abs (28, 29). Of the gp41-reactive mAbs, 11/17 (65%) reacted with ≥1 of 9 non–HIV-1 host proteins and nucleic acids (table S21 and Fig. 2A); 4/17 (23%) reacted with mitochondrial inner membrane lipid component, cardiolipin (table S21), and 5/17 (29%) reacted with HIV-1 uninfected cells (HEp-2 cells) in an immunofluorescence reactivity assay (table S22 and Fig. 2B). We found DNA prime, rAd5-boost, vaccine-induced gp41-reactive Abs to be reactive with WCLs of anaerobic (14/17, 82%) or aerobic (13/17, 76%) IM. Of gp41-reactive Abs, 47% were reactive with the 37-kD subunit of *E. coli* RNA polymerase that has been shown to cross-react with HIV-1 gp41-reactive Abs (2) (Fig. 2C and fig. S11, a and c). In
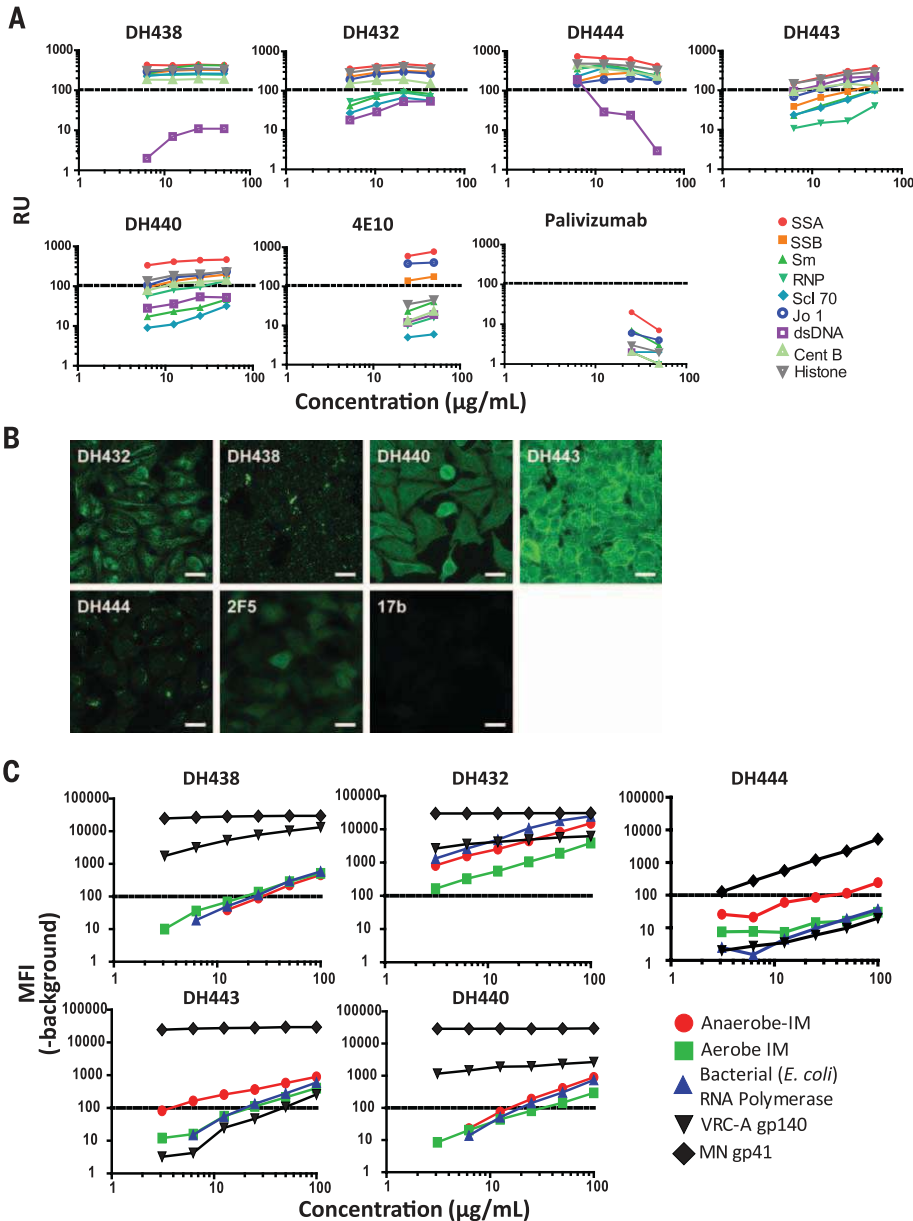
Fig. 2. Polyreactivity of vaccine-induced gp41-reactive mAbs. Five representative polyreactive and gp41-reactive mAbs demonstrated binding with autoantigens [antinuclear Ab (ANA)] (**A**), Hep-2 cells (immunofluorescence staining) (**B**), and anaerobe and aerobe WCLs of IM, bacterial (*E. coli*) RNA polymerase, MN gp41, and vaccine-strain VRC-A gp140 antigens (BAMA) (**C**). (B) All images were taken on an Olympus A×70 fluorescence microscope by using a 40× objective with a SPOT Flex camera. All images were prepared using 50 μg/ml of mAb. Images were acquired for 5 s (2F5 and 17b) or 10 s (DH432, DH438, DH440, DH443, and DH444). Scale bars, 25 μm. (A) and (B) Control Abs: 4E10 (gp41), 2F5 (gp41), 17b (gp41), and palivizumab (RSV). (C) MAb binding was reported as the shift in fluorescence intensity of a population of cells (MFI) versus background versus blank, where background is plate-specific background binding, and blank represents nonspecific sample binding to a negative control bead. Positivity cutoff for binding was 100 MFI, as previously reported (*2*); AbCLL1324 as an IM-reactive control was used to validate IM binding, and gp41 mAb 7B2 that does not react with IM was used as a negative control. Data shown were generated from the same commercially available kits [(A) and (B)], and a single BAMA experiment (C), which was in agreement with Ab-IM reactivity in Western blots (fig. S10 or not shown).

contrast, of the gp120-reactive mAbs, 4/12 (33%) were reactive with ≥1 of 9 host proteins and nucleic acids (table S21), 1/12 (8%) with cardiolipin

(table S21), 1/12 (8%) with HEp-2 cells (table S22), 8/12 (67%) with anaerobic IM-WCLs, 5/12 (42%) with aerobe IM-WCLs, and 2/12 (17%) with *E. coli*

RNA polymerase (fig. S11, b and c). Collectively, DNA prime–rAd5 boost vaccine-induced gp41-reactive mAbs were more polyreactive than gp120-reactive mAbs (*P* < 0.005, Cochran-Mantel-Haenszel test) (Table 2).

NGS of prevaccine IgHV repertoires

The isolation of Abs from HIV-1–infected and naïve individuals that cross-reacted with gp41 and IM-WCLs led to the hypothesis that a pool of B cells exist that are cross-reactive with Env gp41 and IM (*2*, *3*). To determine whether these types of naïve B cells can respond in the setting of HIV-1 Env gp140 vaccination, we performed immunoglobulin variable heavy chain NGS on prevaccination PBMC–derived RNA samples from the eight vaccinees from which postvaccine Env-specific memory B cells were isolated. The immunoglobulin repertoire of *IGHV1-IGHV6* gene families for IgA, G, and M isotypes was probed in prevaccination blood B cells (table S24). We used the V_HDJ_H DNA sequences of all postvaccination Abs with unique V_HDJ_H rearrangements from each of the eight vaccinees to search their prevaccination B cell repertoire for V_HDJ_H rearrangements that belonged to members of the same clonal lineages. We tested the relatedness among sequences by fitting alternative phylogenetic models in which the sequences were or were not hypothesized to share a common ancestor. In both models, we computed a Bayesian average over ancestral sequences; two such ancestors in the model for similar sequences derived from different B cells, one ancestor for the model for clonally related sequences. In the latter case, we also averaged over all unobserved intermediates as well. The model with the larger summed likelihood was selected.

From vaccinee 082-003, we found a prevaccination IgM V_HDJ_H rearrangement (DH477) that was clonally related to a postvaccination gp41-reactive IgG1 Ab, DH476. Direct comparison of these sequences revealed shared junctional sequences, identical HCDR3 length, and 85% HCDR3 nucleotide sequence homology (Fig. 3, A and B, and fig. S12), which demonstrated that prevaccination DH477 and postvaccination DH476 Abs came from the same B cell precursor. In addition to being reactive with all three recombinant vaccine-Envs, the postvaccination Ab DH476 was reactive with rgp41 and with both anaerobe and aerobe IM-WCLs (Fig. 3, C, D, and F). The prevaccine clonal lineage member DH477 was an unmutated IgM Ab complemented by the postvaccine DH476 light chain. Prevaccine Ab DH477 reacted with vaccine strain Env, MN gp41, and host and/or environmental antigens, including IM (Fig. 3, C to F, and tables S25 and S26). The prevaccine Ab DH477 had greater reactivity to IM than the postvaccine Ab DH476 (Fig. 3F) and only bound VRC-A Env surface-expressed on human embryonic kidney 293 (HEK293) cells (Fig. 3E) but did not bind VRC-A, -B, or -C gp140 recombinant proteins (Fig. 3C). Reactivity with IM-WCLs decreased from prevaccination Ab DH477 to postvaccination Ab DH476, whereas increased binding of vaccine Env gp140
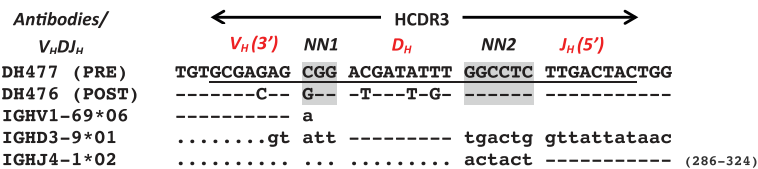
Fig. 3. Characteristics of clonally related Abs. Pre- (DH477) and post- (DH476) vaccine clonally related Abs found in vaccinee 082-003 had the same V_HDJ_H recombination. IGHV, IGHD, and IGHJ Ab segments were statistically inferred (**A** and **B**); nucleotides in the 3′ end of the V-gene and 5′ end of the J-gene shown with rearrangement junctions (gray-shaded nucleotides—NN1, NN2), and HCDR3 (underlined nucleotides) indicated. The lower-case letters show nucleotides that have been removed from the germline gene during V_HDJ_H rearrangement. Pre- (DH477) and post- (DH476) vaccine heavy chain sequences were paired with the natural light chain (IGκV3-20*01, IGκJ1*01, 1.7% mutated nt, 10 amino acid CDR3) of the postvaccine Ab DH476. (**C**) Ab binding to recombinant HIV-1 Env gp140, 5-Helix gp41, and MN gp41 proteins was determined by surface plasmon resonance (SPR) analysis, and (**D**) the Ab binding K_d was determined by rate constants or steady-state analysis measurements. (**E**) Binding of DH477 to VRC-A gp140 expressed on the surface of 293i cells. Anti-V3 mAb (19B) and a representative gp41-reactive Ab (DH440) from this study, both of which bind recombinant VRC-A gp140, were used as positive controls, whereas palivizumab (RSV Ab) was used as a negative IgG1 control. (**F**) The cross-reactivity of pre- (DH477) and post- (DH476) vaccine Abs with intestinal microbiota (IM) whole cell lysates (WCLs) was determined by means of Western blot

A Immunogenetics

PTID	HVTN Trial	Vaccination timepoint	mAb ID	VH	DH	JH	VH mutation frequency (%), nt	HCDR3 length, aa	Ig Isotype
082-003	082	PRE	DH477	1-69*06	3-9*01	4-1*02	0	11	M
		POST	DH476	1-69*06	3-9*01	4-1*02	5.3	11	G

B DH477/DH476_VHDJH junctions

```
                                        ←——————— HCDR3 ———————→
   Antibodies/
   VHDJH              VH (3')    NN1    DH        NN2    JH (5')
DH477 (PRE)   TGTGCGAGAG  CGG  ACGATATTT  GGCCTC  TTGACTACTGG
DH476 (POST)  -------C--  G--  -T---T-G-  ------  -----------
IGHV1-69*06   ----------  a
IGHD3-9*01    ........gt  att  ---------         tgactg gttattataac
IGHJ4-1*02    .........   ...  .........         actact -----------  (286-324)
```

C SPR analysis of DH477 and DH476 binding profile

Binding curves with K_d measurements; relative binding affinities of DH477 and DH476.

E DH477 binding of VRC-A gp145 Env

Control antibodies: positive (+), negative (-)
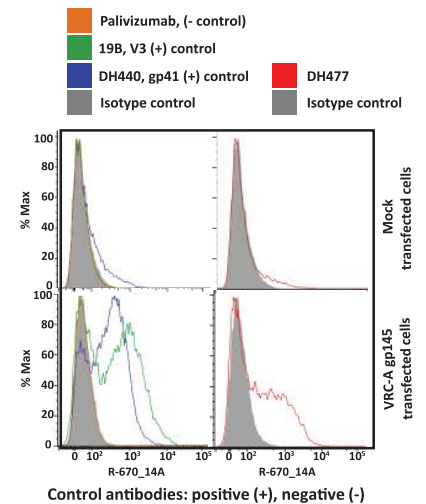
F DH477/DH476 Cross-reactivity profile

SDS-PAGE reduced gels (western blot)

SPR binding data

D DH477/DH476 Antibody binding kinetics

HIV-1 Envelopes	DH477 (pre-vaccine)			DH476 (post-vaccine)		
	k_a, M⁻¹s⁻¹	k_d, s⁻¹	K_d, nM	k_a, M⁻¹s⁻¹	k_d, s⁻¹	K_d, nM
A.92RW020	*nb*	*nb*	*nb*	13x10⁴	4x10⁻⁴	3
B.HxB2/BaL-V3	*nb*	*nb*	*nb*	20x10⁴	3x10⁻⁴	2
C.97ZA012	*nb*	*nb*	*nb*	28x10⁴	34x10⁻⁴	12
M.CON-S	*nb*	*nb*	*nb*	32x10⁴	10x10⁻⁴	3
MN gp41	---	---	41*	10x10³	7x10⁻⁵	7
gp41 5-helix	---	---	21*	2x10⁵	2x10⁻⁴	1

*K_d determined by steady state analysis. nb, no binding.

and SPR as previously described (*2*). DH438 (gp41-reactive Ab) and palivizumab were used as positive and negative control Abs, respectively, for Western blots, and the arrows indicate candidate IM antigens bound by DH476 and/or DH477. In SPR analysis, IM WCLs were diluted in PBS buffer as indicated and injected over mAbs captured on an IgFc-specific Ab immobilized sensor surface. Specific binding of the lysate proteins to the mAbs in SPR were measured after subtraction of nonspecific binding to HA-specific mAb CH65. Abbreviations: nt, nucleotides; aa, amino acid. Data shown in (C) to (F) were representative of duplicate experiments, except SPR screen of DH477 and DH476 for binding rgp140 proteins that was performed once (C).
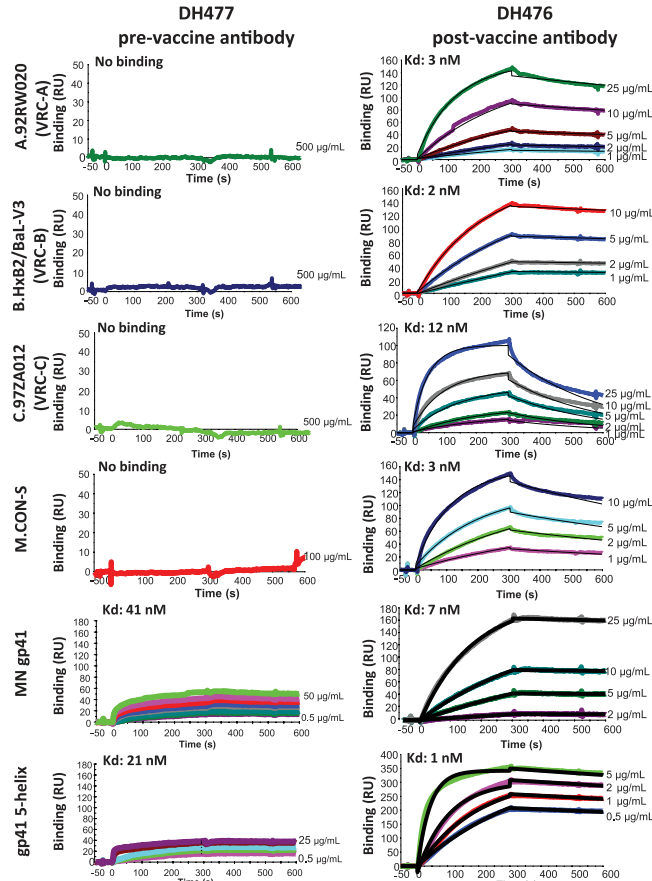
Table 2. Polyreactivity of DNA prime–rAd5 boost vaccine–induced gp41-reactive and gp120-reactive mAbs. Abs were screened for cross-reactivity with anaerobe and aerobe WCLs of IM from human stool and recombinant bacterial (*E. coli*) RNA polymerase (BAMA); host antigens (AtheNA); HEp-2 cells (IFA, indirect fluorescence Ab assay, Zeuss Scientific); and cardiolipin (QUANTA Lite ACA IgG III). *P* values were generated by means of Fisher's exact test (SAS v9.3) or, for all Abs, Cochran-Mantel-Haenszel test controlling for antigen (SAS v9.3).

Antigens	gp41-reactive Abs	gp120-reactive Abs	*P* value
Anaerobe IM	14/17 (82%)	8/12 (67%)	0.40
Aerobe IM	13/17 (76%)	5/12 (42%)	0.12
Bacterial (*E. coli*) RNA polymerase	8/17 (47%)	2/12 (17%)	0.06
AtheNA autoantigen panel	11/17 (65%)	4/12 (33%)	0.14
HEp-2 cells (IFA)	5/17 (29%)	1/12 (8%)	0.35
Cardiolipin	4/17 (24%)	1/12 (8%)	0.63
All antigens tested, gp41-reactive versus gp120-reactive Abs			0.005

and postfusion forms of gp41 was associated with vaccine-Env–induced affinity maturation (Fig. 3, C to F). Thus, vaccine-Env gp41-reactive Ab response can indeed arise from a pool of IM-gp41 cross-reactive B cells that undergo postvaccination affinity maturation.

Discussion

In this study, we found that the DNA prime–rAd5 boost HIV-1 vaccine induced a non-neutralizing dominant Env gp41-reactive Ab response derived from a polyreactive B cell pool. These findings have important implications for HIV-1 vaccine design. The isolation of gp41 and IM-reactive B cells from uninfected individuals (*2, 3*) raised the hypothesis that the HIV-1 gp41-reactive Ab response in HIV-1 infection may in part result from HIV-1 gp41 stimulating a preinfection pool of B cells cross-reactive with IM and Env. We confirmed this hypothesis by the identification of a prevaccination IM, VRC-A gp140, and gp41-reactive Ab that was clonally related to a vaccine-induced Env-reactive Ab (Fig. 3).

The prevaccination gp41-reactive Ab DH477 was an unmutated IgM Ab, which suggested that it represented the receptor of a naïve B cell. Although the great majority of human IgM⁺, IgD⁺ B cells are naïve B cells that are unmutated, a minority of IgM⁺, IgD⁻ memory B cells are unmutated as well (*30, 31*). Thus, DH477 could have been derived from an IgM⁺, IgD⁺ naïve B cell, but we cannot rule out as well that DH477 was derived from an unmutated IgM⁺, IgD⁻ memory B cell. That the pre- (DH477) and post- (DH476) vaccine Abs reacted with IM-WCLs, gp41, and vaccine-Env proteins, suggested that IM or other environmental antigens may stimulate gp41-reactive B cells before vaccination that can react with the vaccine Env but does not prove that all such Abs arose in this manner. B cell development in mice has been demonstrated to occur in the intestinal mucosa and is regulated by extracellular signals from IM that influence the gut immunoglobulin r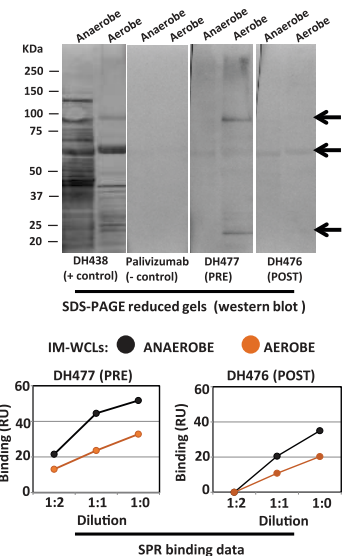epertoire (*32*). Our findings also implicate IM imprinting of B cell development in humans that can affect the quality of an HIV vaccine Ab response.

Here, we demonstrated that an HIV-1 Env-gp140 vaccine containing both gp120 and gp41 primarily induced a gp41-dominant Ab response, whereas previous gp120-only vaccines in humans (*14*) and rhesus macaques (*15*) induced a robust gp120-reactive memory B cell response. It has been demonstrated that B cells with higher affinity for an antigen can outcompete other B cells with lower affinity for the same antigen (*33–35*), and B cells in vitro with similar, but slightly different, B cell receptors can compete for antigen binding (*36*). Thus, our data raise the additional hypothesis that the dominant non-neutralizing IM cross-reactive gp41-reactive Abs outcompeted gp120-reactive Abs.

Of interest, the gp41-reactive Ab response was predominantly restricted to *IGHV1-69* gene segment usage. Previously, IGHV1-69 has been noted for influenza stalk (*20, 37*), HIV-1 gp41 hydrophobic pocket (*21*), and membrane-proximal region Ab responses (*38*). That the gp41 Ab response constituted predominantly IGHV1-69 memory B cells that used the 54L-HCDR2 IGHV1-69 alleles suggested that the 54L-HCDR2 *IGHV1-69* gene allele variant was the predominant IGHV better able to structurally recognize the dominant gp41 epitope expressed by the DNA prime–rAd5 boost vaccine. However, it is important to note that prevaccine Ab DH477 used the 54F-HCDR2 variant of IGHV1-69 (Fig. 3 and fig. S12), whereas the clonally related postvaccine Ab DH476 used the 54L IGHV1-69 variant (table S5 and fig. S12). Thus, a second mechanism of 54L VH1-69 usage was via somatic hypermutations to recognize gp41 epitopes presented by gp140 immunogens in the DNA prime–rAd5 boost vaccine.

One hypothesis for vaccine optimization is to use a native trimer containing gp41 to attempt to induce broadly reactive neutralizing Abs (bnAbs) (*39, 40*). These immunogens contain the recently described gp41-gp120 conformational bnAbs epitopes (*41–44*) but not the membrane-proximal portion of gp41-neutralizing epitopes (*45, 46*). The Env insert in the VRC Env DNA-Ad5 vaccine had a partial deletion in the C-C loop of gp41, unlike the native Env. Although it has been

reported that another HIV-1 Env vaccine with the gp41 C-C loop intact has also induced high levels of gp41-reactive Abs (*47*), this vaccine has not been studied in an efficacy trial, nor have its vaccine-induced gp41-reactive mAbs been characterized, not even for environmental or IM cross-reactivity. In nonhuman primate studies, gp41-reactive plasma Abs have been reported to be both protective (*48, 49*) and nonprotective (*50, 51*). Defining the B cell compartment from which polyreactive gp41-reactive B cells originate and determining how they are regulated are important areas of future study. The low proportion of gp120 Abs does not exclude the possibility that additional Abs were generated against other forms of the ectodomain, for example, conformational epitopes. Future studies will evaluate this possibility.

Thus, as in HIV-1 infection, Env vaccination can induce polyreactive, non-neutralizing gp41-reactive Ab repertoire responses from preexisting B cells that can be cross-reactive with IM. Because the B cell repertoire can be imprinted at birth by IM antigens (*32*), our data raise the hypothesis that neonatal immunization with HIV-1 Env may be able to imprint the B cell repertoire to respond to Env antigenic sites that may otherwise be subdominant or disfavored, including Env broadly neutralizing Ab epitopes (*52, 53*). In this regard, Goo *et al.* recently reported that HIV-1–infected infants can make broadly neutralizing Abs, and in some cases, such Abs arise within the first year of life (*54*).

Finally, if similar diversion toward dominant polyreactive gp41-reactive Abs is found with other gp41-containing vaccine regimens with intact gp41, the data in this study suggest that one region of gp41 in vaccine immunogens that might be considered for deletion or modification to avoid IM-gp41 cross-reactivity in the setting of vaccination includes amino acids in the gp41 HR-1 region.

Materials and methods
Clinical trial samples

Vaccine-induced Ab repertoires were studied 4 weeks after final vaccination (rAd5 boost) in plasma and blood-derived memory B cells of four HVTN 204 (*5*), and four HVTN 082 (Protocol HVTN 082; DIADS Document ID 10771) trial participants, as well as in plasma only from an additional 40 HVTN 505 vaccine recipients (*11*). Vaccinees were HIV-1 seronegative adults enrolled in the phase Ib HVTN 082 (Protocol HVTN 082; DIADS Document ID 10771) and phase II HVTN 204 (Protocol HVTN 204; BB IND 12326 HELD BY DAIDS) (*5*) trials that studied the DNA prime–rAd5 boost vaccine. From *n* = 480 (HVTN 204), the four participants chosen for our study displayed plasma binding reactivity with vaccine strain Envs, and/or neutralization of clade C MW965 HIV-1 isolate. From *n* = 8 (HVTN 082, four twin pairs), we selected one individual from each twin pair to study genetically different subjects. All study samples were obtained by informed consent, and all studies were approved by the Duke University Institutional Review Board.

Flow cytometry memory B cell single-cell sorting

Single-cell isolation of memory B cells decorated with both AlexaFluor 647 and Brilliant Violet 421–tagged HIV-1 VRC-A (A.92RW020), VRC-B (B.HxB2/BaL-V3), VRC-C (C.97ZA012), or CON-S Env gp140s or gp120s was performed using a fluorescence-activated cell sorter, either FACSAria or FACSAria II (BD Biosciences, San Jose, CA), and the flow cytometry data were analyzed using FlowJo (Treestar, Ashland, OR) (13, 14, 55).

Ab binding and epitope mapping

Recombinant mAbs were screened for binding specificities to multiclade HIV-1 gp120 Envs and clade B.MN gp41 (Product 10911, ImmunoDX, Woburn, MA) by means of standard ELISA (56). Gp120-reactive Abs bound both Env gp140 and gp120 recombinant proteins, but gp41-reactive Abs bound recombinant MN gp41 protein or differentially to CON-S and/or VRC A Envs (CON-S gp140+, CON-S gp120–; VRC-A gp140+, VRC-A gp120–). MAbs were epitope-mapped on multiclade consensus and primary isolates gp140 overlapping peptide sets, including HIV-1 MN and B.CON gp140 obtained from the NIH AIDS Reagent Repository, by means of ELISA and linear peptide array (57). The binding Ab multiplex assay (BAMA)—a standardized custom binding Ab multiplex assay—was used to determine reactivity of serum and recombinant mAbs with antigens (1). Prevaccinated serum samples and a respiratory syncytial virus (RSV)–specific mAb (palivizumab) were used to establish plasma and mAb binding cutoffs, respectively, in BAMA. For SPR analysis, Env gp140 (A.92RW020, B.HxB2/Bal, C.97ZA012, or M.CON-S), 5-helix gp41 (21), and MN gp41 proteins (Product 10911, ImmunoDX) binding was measured by injecting Env proteins at varying concentration (0.5 to 500 μg/ml) over each mAb captured on human IgFc–specific immobilized Ab (Millipore) on a CM5 sensor surface as previously described (58). Nonspecific binding to the control palivizumab mAb and signal drifts from phosphate-buffered saline (PBS) were used for double referencing and to measure specific binding responses. Rate constants for association and dissociation (k_a and k_d, respectively) were measured by global curve fitting to a 1:1 Langmuir model as described previously (58). For gp41 proteins (MN gp41 and 5-helix) binding to prevaccine Abs, rate constants could not be reliably measured because of saturation of binding responses at relatively lower antigen concentrations, and values for the dissociation constant (K_d) were measured using steady-state analysis. Postvaccine Abs did not show this limitation when binding to either MN gp41 or 5-helix gp41 proteins (Fig. 3).

Ab staining of cell surface–expressed HIV-1 VRC-A gp145

For the surface expression of VRC-A gp145, HEK293i cells were transfected with pHV130770 plasmids using ExpiFectamine 293 Transfection Kits (Life Technologies, A14525, Grand Island, NY) following the manufacturers' protocol. The cells were washed with four volumes of room-temperature phosphate-buffered saline (DPBS) (Life Technologies 10010-023) and centrifuged (500g for 5 min). Cells (10^6) were resuspended in 80 μl of staining buffer (1% BSA in DPBS) to which were added 20 μl of diluted Abs (1 μg per reaction). After incubation (1 hour at 4°C) with shaking, cells were washed and centrifuged (500g). Cells were incubated with either 20 μl isotype-APC control (BD cat. 555751) or 20 μl human IgG-APC–specific (BD cat 550931) for 30 to 45 min at 4°C, protected from light. After washing and fixation, cells were analyzed by flow cytometer (BD LSRFortessa).

Ab polyreactivity

Vaccine-induced polyreactivity of Abs was assessed by using commercially available kits (AtheNA Multi-Lyte System and HEp-2 cell immunofluorescence assay, Zeus Scientific; anticardiolipin ELISA - QUANTA Lite ACA IgG III, Inova Diagnostics, San Diego, CA) (3). Reactivity with WCLs of anaerobic and aerobic IM extracts of stool specimens (3) was determined by using BAMA and Western blot (WB), as described previously (2). For WB analysis, 20 μg/ml of mAbs was used to test reactivity with 100 μg of IM WCLs. SPR analysis of IM WCL samples was performed on a BIAcore 3000 instrument (GE Healthcare), as previously described (2), with some modifications. IM WCL samples were spun down to remove aggregates, and each lysate sample (total protein concentrations of 7.87 and 7.97 mg/ml for aerobic and anaerobic lysates, respectively) was diluted in PBS buffer (1:1 or 1:2) and injected over each mAb captured over a human IgFc–specific Ab immobilized on a C1 sensor chip. Specific binding of the lysate proteins to the mAbs was measured after subtraction of nonspecific binding to HA-specific mAb CH65, and binding responses were measured at post-injection report point (10 s after injection).

Proteomic analysis of IM proteins and HIV-1 VRC-A gp140

SDS-PAGE gels were run with IM proteins, and Western blot analysis was performed with three VRC-A gp140 and MN gp41-reactive, IM cross-reactive IGHV1-69–using mAbs: DH440, DH432, and DH438. Bands were cut from gels that were reactive with one or more of these mAbs in Western blot, and we performed proteomic analysis by LC-MS of tryptic fragments of these protein bands to identify the reactive protein. One of these bands (An1) was recognized by all three gp41-reactive mAbs, and an identified protein in the WB-reactive band An1 (fig. S10) was bacterial pyruvate-flavodoxin oxidoreductase (National Center for Biotechnology Information, NIH, accession no: WP_022497386).

In order to directly determine where on the VRC-A gp140 protein the vaccine-induced gp41 mAbs bound, we proteolytically cleaved the gp140 protein with trypsin and then analyzed the cleavage products by WB analysis. One of the reactive bands (~25 kD) that blotted with the gp41-reactive mAb tested was identified by LC-MS proteomic analysis after reduction and alkylation.

Sequence and structural similarities of HIV-1 Env gp41 and bacterial proteins

Alignment of bacterial protein identified by LC-MS with gp41 Env sequences was assessed by BLAST analysis of the VRC-A, VRC-B, and VRC-C gp140 and MN gp41 amino acid sequences against sequences of 19 candidate proteins identified in IM by LC-MS. We used a cutoff E-value of <1 to allow for short stretches of sequence matches. The BLAST search returned only one similar region in pyruvate flavodoxin oxidoreductase, where sequence similarity was observed below the E-value cutoff between bacterial proteins and the gp41 ectodomain. The H1 helices at the homodimer interface of the α subunit of RNA polymerase (PDB: 1BDF) were structurally aligned to the six-helix bundle conformation of gp41 (PDB: 1AIK), by using an implementation of the Kabsch algorithm.

Ab functional characterization

Purified mAbs were screened for neutralization by means of TZM-bl assay (59, 60), ADCC (61, 62), and infectious virion capture (63) of HIV-1 isolates.

PCR isolation of heavy and light chain genes

Heavy (IGHV) and light (IGKV, IGLV) chain genes were isolated by means of single-cell PCR (13, 64), and the sequences were computationally determined as described (65–67). Inferences of the genetic features of the immunoglobulin IGHV, IGKV, and IGLV sequences were previously described (68, 69).

Expression of IGHV, IGKV, and IGLV chains as full-length IgG1 rmAbs

Plasmids encoding the IGHV, IGKV, and IGLV genes were generated and used for recombinant monoclonal Ab (rmAb) production in human embryonic kidney cell lines (ATCC, Manassas, VA) (13, 38), by means of small-scale transfection and as purified mAbs in larger quantities (70, 71). Purified rmAbs were dialyzed against PBS, analyzed, and stored at 4°C.

Clonal lineage determination

Sequences were subject to statistical analysis for lineage membership. Briefly, sequences were organized into clans, by definition sharing inferred IGHV and IGHJ genes and CDRH3 length. Within these clans, we used agglomerative clustering using a Bayesian phylogenetic merit function as follows. To calculate the score for the hypothesis that a given sequence is a member of a lineage L, we compute the posterior likelihoods under the phylogenetic hypotheses that they are and are not members of the same clone. The Bayes factor for this comparison is the objective function for clustering. Sequences were taken in succession and placed into the lineage (including an empty lineage, i.e., founding a new lineage) that maximizes the objective function. The automated inference was followed up by visual inspection of the DNA sequence alignments for confirmation.

Statistical analysis

Statistically significant differences in the profiles of gp120-reactive and gp41-reactive Abs were determined by means of various tests (as indicated for each table and figure) in SAS software (SAS v9.3). A $P < 0.05$ determined statistical significance.

NGS

PBMC-extracted RNA was used to generate cDNA amplicons for pyrosequencing (Illumina). RNA isolated from vaccinee PBMCs was separated into two equal aliquots before cDNA production; cDNA amplification and NGS were performed on both aliquots as independent samples. *IGHV* genes were amplified by means of a modification of the processes previously described (*13*). The reverse transcription (RT) reaction was carried out in 30-μl reaction mixtures at 55°C for 1 hour after addition of 50 units/reaction of Superscript III reverse transcriptase (Invitrogen, Carlsbad, CA), 40 units/reaction of RNaseOUT (Invitrogen), 25 mM deoxynucleotide triphosphates (dNTPs) (Invitrogen), 5× first strand buffer (Invitrogen), 0.1 mM DTT (Invitrogen), and 25 μM human IgA, IgG, and IgM constant region primers as previously described (*13*). After cDNA synthesis, *IGHV1-IGHV6* genes were amplified separately for IgA, IgG, and IgM isotypes by two rounds of PCR in 96-well PCR plates in 50 μl reaction mixtures. The first-round of PCR contained 5 μl of RT reaction products, 1 unit of iProof DNA polymerase (Biorad), 10 μl 5× iProof GC buffer (Biorad), 10 mM dNTPs (Invitrogen), 50 mM MgCl₂ (Biorad), and 25 μM of IgA, IgG, or IgM constant region primers and sets of IGHV-IGHV6 variable region primers (table S23). The first round of PCR was performed at 98°C ×1 min followed by 25 cycles of 98°C ×15 s, 60°C ×15 s, 72°C ×35 s, and one cycle at 72°C ×7 min. First-round PCR products were purified by using a QIAquick PCR purification kit (Qiagen) and eluted into 50 μl of DNase/RNase-free distilled water. Nested second-round PCR was performed in 50 μl of reaction mixture with 5 μl of purified first-round PCR product, 1.25 units/reaction Platinum *Taq* DNA Polymerase High Fidelity (Invitrogen), 10 mM dNTPs, and 5 μl of Nextera index kit barcode-tagged primers (Illumina). During the second round of nested PCR, the IGHV1-IGHV6 primers were amplified in separate reaction mixes for each variable region primer. The second round of PCR was performed at 94°C ×2 min followed by three cycles of 94°C ×15 s, 55°C ×30 s, 68°C ×30 s; seven cycles of 94°C ×15 s, 60°C ×30 s, 68°C ×30 s; and one cycle at 68°C ×10 min. Samples of IGHV chain PCR products were analyzed on 2% agarose gels before total sample purification by means of gel extraction (QIAquick gel extraction kit; Qiagen) and eluted into 25 μl of DNase/RNase-free distilled water. IGHV1-IGHV6 cDNA amplicons (5 μl) were pooled for each immunoblobulin isotype. Pooled IgA, IgG, and IgM cDNA amplicons were quantified using the KAPA SYBR FAST qPCR kit (KAPA Biosystems). IgA, IgG, and IgM samples at 4 nM were selected for NGS. IgA, IgG, and IgM samples were denatured with NaOH (1×) and then mixed with hybridization buffer. Denatured samples were mixed

with 35% (by volume) PhiX control/nonrelevant DNA (Illumina) in a final reaction mixture, from which 600 μl were loaded to Illumina MiSeq kit v3 for 600 cycles of PCR amplification. We have previously shown that the primer set used here does not induce primer IGHV bias (*3*).

NGS-generated sequences were processed and analyzed computationally according to the following protocol; Illumina reads were discarded if they did not meet the following criteria: ≥30 Phred quality score (corresponding to 99.9% base call accuracy) for at least 95% of all base positions in the sequence. Primer sequences were removed from the reads, and only unique sequences were retained. The unique sequences were then analyzed using the Cloanalyst software suite (*72*) to infer the IGHV rearrangements (V_HDJ_H) and to determine clonal relatedness. Illumina NGS was performed independently on duplicate samples (RNA samples split into two aliquots for independent cDNA production, amplification, and deep sequencing). Illumina runs were performed with independent Illumina kits. For the purpose of gene counting, only sequences that appeared in both duplicate runs (no mismatches in the coding region) were used (tables S12 and S24). For the identification of prevaccine lineage members, replication was not required. The statistical methods we used are not sensitive to random sequencing error, and the likelihood that sequencing errors would produce artifactual apparent lineage membership in an otherwise unrelated sequence is negligible.

We used NGS to study the prevaccination samples of all eight vaccinees in the study, and we found three vaccinees whose prevaccination samples had Abs that were in the same Ab clan (same V_HDJ_H and HCDR3 length and similarity), but two of these prevaccination Abs had ambiguities in their junctional sequences and shared mutations versus allelic differences, such that a definitive conclusion could not be reached that the prevaccination and postvaccination V_HDJ_H originated from the same B cell. However, in the case of the prevaccination DH477 and postvaccination DH476 Abs, from the shared mutations and junctional sequences, we could definitively state that they arose from the same B cell. In order to investigate the binding specificities of the pre- (DH477) and post (DH476) vaccine Abs, pre- and postvaccine V_H chains were paired with the natural light chain of the postvaccine Ab.

REFERENCES AND NOTES

1. G. D. Tomaras *et al.*, Initial B-cell responses to transmitted human immunodeficiency virus type 1: Virion-binding immunoglobulin M (IgM) and IgG antibodies followed by plasma anti-gp41 antibodies with ineffective control of initial viremia. *J. Virol.* **82**, 12449–12463 (2008). doi: 10.1128/JVI.01708-08; pmid: 18842730
2. A. M. Trama *et al.*, HIV-1 envelope gp41 antibodies can originate from terminal ileum B cells that share cross-reactivity with commensal bacteria. *Cell Host Microbe* **16**, 215–226 (2014). doi: 10.1016/j.chom.2014.07.003; pmid: 25121750
3. H. X. Liao *et al.*, Initial antibodies binding to HIV-1 gp41 in acutely infected subjects are polyreactive and highly mutated. *J. Exp. Med.* **208**, 2237–2249 (2011). doi: 10.1084/jem.20110363; pmid: 21987658
4. A. T. Catanzaro *et al.*, Phase I clinical evaluation of a six-plasmid multiclade HIV-1 DNA candidate vaccine. *Vaccine* **25**,

4085–4092 (2007). doi: 10.1016/j.vaccine.2007.02.050; pmid: 17391815
5. G. J. Churchyard *et al.*, A phase IIA randomized clinical trial of a multiclade HIV-1 DNA prime followed by a multiclade rAd5 HIV-1 vaccine boost in healthy adults (HVTN204). *PLOS ONE* **6**, e21225 (2011). doi: 10.1371/journal.pone.0021225; pmid: 21857901
6. H. Kibuuka *et al.*, A phase 1/2 study of a multiclade HIV-1 DNA plasmid prime and recombinant adenovirus serotype 5 boost vaccine in HIV-Uninfected East Africans (RV 172). *J. Infect. Dis.* **201**, 600–607 (2010). doi: 10.1086/650299; pmid: 20078213
7. W. Jaoko *et al.*, Safety and immunogenicity study of Multiclade HIV-1 adenoviral vector vaccine alone or as boost following a multiclade HIV-1 DNA vaccine in Africa. *PLOS ONE* **5**, e12873 (2010). doi: 10.1371/journal.pone.0012873; pmid: 20877623
8. B. S. Graham *et al.*, Phase 1 safety and immunogenicity evaluation of a multiclade HIV-1 DNA candidate vaccine. *J. Infect. Dis.* **194**, 1650–1660 (2006). doi: 10.1086/509259; pmid: 17109336
9. A. T. Catanzaro *et al.*, Phase 1 safety and immunogenicity evaluation of a multiclade HIV-1 candidate vaccine delivered by a replication-defective recombinant adenovirus vector. *J. Infect. Dis.* **194**, 1638–1649 (2006). doi: 10.1086/509258; pmid: 17109335
10. R. A. Koup *et al.*, Priming immunization with DNA augments immunogenicity of recombinant adenoviral vectors for both HIV-1 specific antibody and T-cell responses. *PLOS ONE* **5**, e9015 (2010). doi: 10.1371/journal.pone.0009015; pmid: 20126394
11. S. M. Hammer *et al.*, Efficacy trial of a DNA/rAd5 HIV-1 preventive vaccine. *N. Engl. J. Med.* **369**, 2083–2092 (2013). doi: 10.1056/NEJMoa1310566; pmid: 24099601
12. H. X. Liao *et al.*, A group M consensus envelope glycoprotein induces antibodies that neutralize subsets of subtype B and C HIV-1 primary viruses. *Virology* **353**, 268–282 (2006). doi: 10.1016/j.virol.2006.04.043; pmid: 17039602
13. H. X. Liao *et al.*, High-throughput isolation of immunoglobulin genes from single human B cells and expression as monoclonal antibodies. *J. Virol. Methods* **158**, 171–179 (2009). doi: 10.1016/j.jviromet.2009.02.014; pmid: 19428587
14. M. A. Moody *et al.*, HIV-1 gp120 vaccine induces affinity maturation in both new and persistent antibody clonal lineages. *J. Virol.* **86**, 7496–7507 (2012). doi: 10.1128/JVI.00426-12; pmid: 22553329
15. K. Wiehe *et al.*, Antibody light-chain-restricted recognition of the site of immune pressure in the RV144 HIV-1 vaccine trial is phylogenetically conserved. *Immunity* **41**, 909–918 (2014). doi: 10.1016/j.immuni.2014.11.014; pmid: 25526306
16. S. D. Boyd *et al.*, Individual variation in the germline Ig gene repertoire inferred from variable region gene rearrangements. *J. Immunol.* **184**, 6986–6992 (2010). doi: 10.4049/jimmunol.1000445; pmid: 20495067
17. E. H. Sasso, T. Johnson, T. J. Kipps, Expression of the immunoglobulin VH gene 51p1 is proportional to its germline gene copy number. *J. Clin. Invest.* **97**, 2074–2080 (1996). doi: 10.1172/JCI118644; pmid: 8621797
18. 1000 Genomes Project Consortium, A map of human genome variation from population-scale sequencing. *Nature* **467**, 1061–1073 (2010). doi: 10.1038/nature09534; pmid: 20981092
19. R. A. Lerner, Rare antibodies from combinatorial libraries suggests an S.O.S. component of the human immunological repertoire. *Mol. Biosyst.* **7**, 1004–1012 (2011). doi: 10.1039/c0mb00310g; pmid: 21298133
20. R. Xu *et al.*, A recurring motif for antibody recognition of the receptor-binding site of influenza hemagglutinin. *Nat. Struct. Mol. Biol.* **20**, 363–370 (2013). doi: 10.1038/nsmb.2500; pmid: 23396351
21. M. A. Luftig *et al.*, Structural basis for HIV-1 neutralization by a gp41 fusion intermediate-directed antibody. *Nat. Struct. Mol. Biol.* **13**, 740–747 (2006). doi: 10.1038/nsmb1127; pmid: 16862157
22. C. Sabin *et al.*, Crystal structure and size-dependent neutralization properties of HK20, a human monoclonal antibody binding to the highly conserved heptad repeat 1 of gp41. *PLOS Pathog.* **6**, e1001195 (2010). doi: 10.1371/journal.ppat.1001195; pmid: 21124990
23. K. K. Hwang *et al.*, IGHV1-69 B cell chronic lymphocytic leukemia antibodies cross-react with HIV-1 and hepatitis C virus antigens as well as intestinal commensal bacteria. *PLOS ONE* **9**, e90725 (2014). doi: 10.1371/journal.pone.0090725; pmid: 24614505
24. M. A. Moody *et al.*, H3N2 influenza infection elicits more cross-reactive and less clonally expanded anti-hemagglutinin

antibodies than influenza vaccination. *PLOS ONE* **6**, e25797 (2011). doi: 10.1371/journal.pone.0025797; pmid: 22039424

25. N. Darzentas *et al.*, A different ontogenesis for chronic lymphocytic leukemia cases carrying stereotyped antigen receptors: Molecular and computational evidence. *Leukemia* **24**, 125–132 (2010). doi: 10.1038/leu.2009.186; pmid: 19759557

26. D. C. Chan, D. Fass, J. M. Berger, P. S. Kim, Core structure of gp41 from the HIV envelope glycoprotein. *Cell* **89**, 263–273 (1997). doi: 10.1016/S0092-8674(00)80205-6; pmid: 9108481

27. G. Zhang, S. A. Darst, Structure of the *Escherichia coli* RNA polymerase alpha subunit amino-terminal domain. *Science* **281**, 262–266 (1998). doi: 10.1126/science.281.5374.262; pmid: 9657722

28. H. Mouquet, M. C. Nussenzweig, Polyreactive antibodies in adaptive immune responses to viruses. *Cell. Mol. Life Sci.* **69**, 1435–1445 (2012). doi: 10.1007/s00018-011-0872-6; pmid: 22045557

29. B. F. Haynes *et al.*, Cardiolipin polyspecific autoreactivity in two broadly neutralizing HIV-1 antibodies. *Science* **308**, 1906–1908 (2005). doi: 10.1126/science.1111781; pmid: 15860590

30. U. Klein, R. Küppers, K. Rajewsky, Evidence for a large compartment of IgM-expressing memory B cells in humans. *Blood* **89**, 1288–1298 (1997).pmid: 9028952

31. U. Klein, R. Küppers, K. Rajewsky, Human IgM+IgD+ B cells, the major B cell subset in the peripheral blood, express V_χ genes with no or little somatic mutation throughout life. *Eur. J. Immunol.* **23**, 3272–3277 (1993). doi: 10.1002/eji.1830231232; pmid: 8258343

32. D. R. Wesemann *et al.*, Microbial colonization influences early B-lineage development in the gut lamina propria. *Nature* **501**, 112–115 (2013). doi: 10.1038/nature12496; pmid: 23965619

33. J. M. Dal Porto, A. M. Haberman, G. Kelsoe, M. J. Shlomchik, Very low affinity B cells form germinal centers, become memory B cells, and participate in secondary immune responses when higher affinity competition is reduced. *J. Exp. Med.* **195**, 1215–1221 (2002). doi: 10.1084/jem.20011550; pmid: 11994427

34. T. A. Y. Shih, E. Meffre, M. Roederer, M. C. Nussenzweig, Role of BCR affinity in T cell dependent antibody responses in vivo. *Nat. Immunol.* **3**, 570–575 (2002). doi: 10.1038/ni803; pmid: 12021782

35. J. M. Dal Porto, A. M. Haberman, M. J. Shlomchik, G. Kelsoe, Antigen drives very low affinity B cells to become plasmacytes and enter germinal centers. *J. Immunol.* **161**, 5373–5381 (1998). pmid: 9820511

36. A. T. McGuire *et al.*, Antigen modification regulates competition of broad and narrow neutralizing HIV antibodies. *Science* **346**, 1380–1383 (2014). doi: 10.1126/science.1259206; pmid: 25504724

37. J. Sui *et al.*, Structural and functional bases for broad-spectrum neutralization of avian and human influenza A viruses. *Nat. Struct. Mol. Biol.* **16**, 265–273 (2009). doi: 10.1038/nsmb.1566; pmid: 19234466

38. L. Morris *et al.*, Isolation of a human anti-HIV gp41 membrane proximal region neutralizing antibody by antigen-specific single B cell sorting. *PLOS ONE* **6**, e23532 (2011). doi: 10.1371/journal.pone.0023532; pmid: 21980336

39. J. P. Julien *et al.*, Crystal structure of a soluble cleaved HIV-1 envelope trimer. *Science* **342**, 1477–1483 (2013). doi: 10.1126/science.1245625; pmid: 24179159

40. D. Lyumkis *et al.*, Cryo-EM structure of a fully glycosylated soluble cleaved HIV-1 envelope trimer. *Science* **342**, 1484–1490 (2013). doi: 10.1126/science.1245627; pmid: 24179160

41. E. Falkowska *et al.*, Broadly neutralizing HIV antibodies define a glycan-dependent epitope on the prefusion conformation of gp41 on cleaved envelope trimers. *Immunity* **40**, 657–668 (2014). doi: 10.1016/j.immuni.2014.04.009; pmid: 24768347

42. C. Blattner *et al.*, Structural delineation of a quaternary, cleavage-dependent epitope at the gp41-gp120 interface on intact HIV-1 Env trimers. *Immunity* **40**, 669–680 (2014). doi: 10.1016/j.immuni.2014.04.008; pmid: 24768348

43. L. Scharf *et al.*, Antibody 8ANC195 reveals a site of broad vulnerability on the HIV-1 envelope spike. *Cell Reports* **7**, 785–795 (2014). doi: 10.1016/j.celrep.2014.04.001; pmid: 24767986

44. J. Huang *et al.*, Broad and potent HIV-1 neutralization by a human antibody that binds the gp41-gp120 interface. *Nature* **515**, 138–142 (2014). doi: 10.1038/nature13601; pmid: 25186731

45. T. Muster *et al.*, Cross-neutralizing activity against divergent human immunodeficiency virus type 1 isolates induced by the gp41 sequence ELDKWAS. *J. Virol.* **68**, 4031–4034 (1994). pmid: 7514684

46. J. Huang *et al.*, Broad and potent neutralization of HIV-1 by a gp41-specific human antibody. *Nature* **491**, 406–412 (2012). doi: 10.1038/nature11544; pmid: 23151583

47. P. A. Goepfert *et al.*, Specificity and 6-month durability of immune responses induced by DNA and recombinant modified vaccinia Ankara vaccines expressing HIV-1 virus-like particles. *J. Infect. Dis.* **210**, 99–110 (2014). doi: 10.1093/infdis/jiu003; pmid: 24403557

48. Q. Li *et al.*, Live simian immunodeficiency virus vaccine correlate of protection: Local antibody production and concentration on the path of virus entry. *J. Immunol.* **193**, 3113–3125 (2014). doi: 10.4049/jimmunol.1400820; pmid: 25135832

49. H. L. Robinson, Non-neutralizing antibodies in prevention of HIV infection. *Expert Opin. Biol. Ther.* **13**, 197–207 (2013). doi: 10.1517/14712598.2012.743527; pmid: 23130709

50. D. R. Burton *et al.*, Limited or no protection by weakly or nonneutralizing antibodies against vaginal SHIV challenge of macaques compared with a strongly neutralizing antibody. *Proc. Natl. Acad. Sci. U.S.A.* **108**, 11181–11186 (2011). doi: 10.1073/pnas.1103012108; pmid: 21690411

51. S. Kwa *et al.*, CD40L-adjuvanted DNA/modified vaccinia virus Ankara simian immunodeficiency virus (SIV) vaccine enhances protection against neutralization-resistant mucosal SIV infection. *J. Virol.* **89**, 4690–4695 (2015). doi: 10.1128/JVI.03527-14; pmid: 25653428

52. B. F. Haynes, L. Verkoczy, AIDS/HIV. Host controls of HIV neutralizing antibodies. *Science* **344**, 588–589 (2014). doi: 10.1126/science.1254990; pmid: 24812389

53. G. D. Tomaras, B. F. Haynes, Lessons from babies: Inducing HIV-1 broadly neutralizing antibodies. *Nat. Med.* **20**, 583–585 (2014). doi: 10.1038/nm.3598; pmid: 24901564

54. L. Goo, V. Chohan, R. Nduati, J. Overbaugh, Early development of broadly neutralizing antibodies in HIV-infected infants. *Nat. Med.* **20**, 655–658 (2014). doi: 10.1038/nm.3565; pmid: 24859529

55. E. S. Gray *et al.*, Isolation of a monoclonal antibody that targets the alpha-2 helix of gp120 and represents the initial autologous neutralizing-antibody response in an HIV-1 subtype C-infected individual. *J. Virol.* **85**, 7719–7729 (2011). doi: 10.1128/JVI.00563-11; pmid: 21613396

56. H. X. Liao *et al.*, Vaccine induction of antibodies against a structurally heterogeneous site of immune pressure within HIV-1 envelope protein variable regions 1 and 2. *Immunity* **38**, 176–186 (2013). doi: 10.1016/j.immuni.2012.11.011; pmid: 23313589

57. J. Friedman *et al.*, Isolation of HIV-1-neutralizing mucosal monoclonal antibodies from human colostrum. *PLOS ONE* **7**, e37648 (2012). doi: 10.1371/journal.pone.0037648; pmid: 22624058

58. S. M. Alam *et al.*, Antigenicity and immunogenicity of RV144 vaccine AIDSVAX clade E envelope immunogen is enhanced by a gp120 N-terminal deletion. *J. Virol.* **87**, 1554–1568 (2013). doi: 10.1128/JVI.00718-12; pmid: 23175357

59. D. C. Montefiori *et al.*, Magnitude and breadth of the neutralizing antibody response in the RV144 and Vax003 HIV-1 vaccine efficacy trials. *J. Infect. Dis.* **206**, 431–441 (2012). doi: 10.1093/infdis/jis367; pmid: 22634875

60. E. S. Gray *et al.*, Broad neutralization of human immunodeficiency virus type 1 mediated by plasma antibodies against the gp41 membrane proximal external region. *J. Virol.* **83**, 11265–11274 (2009). doi: 10.1128/JVI.01359-09; pmid: 19692477

61. J. Pollara *et al.*, High-throughput quantitative analysis of HIV-1 and SIV-specific ADCC-mediating antibody responses. *Cytometry A* **79A**, 603–612 (2011). doi: 10.1002/cyto.a.21084; pmid: 21735545

62. M. Bonsignori *et al.*, Antibody-dependent cellular cytotoxicity-mediating antibodies from an HIV-1 vaccine efficacy trial target multiple epitopes and preferentially use the VH1 gene family. *J. Virol.* **86**, 11521–11532 (2012). doi: 10.1128/JVI.01023-12 pmid: 22896626

63. P. Liu *et al.*, Infectious virion capture by HIV-1 gp120-specific IgG from RV144 vaccinees. *J. Virol.* **87**, 7828–7836 (2013). doi: 10.1128/JVI.02737-12; pmid: 23658446

64. K. Smith *et al.*, Rapid generation of fully human monoclonal antibodies specific to a vaccinating antigen. *Nat. Protoc.* **4**, 372–384 (2009). doi: 10.1038/nprot.2009.3; pmid: 19247287

65. B. Ewing, P. Green, Base-calling of automated sequencer traces using *phred*. II. Error probabilities. *Genome Res.* **8**, 186–194 (1998). doi: 10.1101/gr.8.3.175; pmid: 9521922

66. B. Ewing, L. Hillier, M. C. Wendl, P. Green, Base-calling of automated sequencer traces using *phred*. I. Accuracy assessment. *Genome Res.* **8**, 175–185 (1998). doi: 10.1101/gr.8.3.175; pmid: 9521921

67. T. B. Kepler *et al.*, Chiropteran types I and II interferon genes inferred from genome sequencing traces by a statistical gene-family assembler. *BMC Genomics* **11**, 444 (2010). doi: 10.1186/1471-2164-11-444; pmid: 20663124

68. T. F. Smith, M. S. Waterman, Identification of common molecular subsequences. *J. Mol. Biol.* **147**, 195–197 (1981). doi: 10.1016/0022-2836(81)90087-5; pmid: 7265238

69. J. M. Volpe, L. G. Cowell, T. B. Kepler, SoDA: Implementation of a 3D alignment algorithm for inference of antigen receptor recombinations. *Bioinformatics* **22**, 438–444 (2006). doi: 10.1093/bioinformatics/btk004; pmid: 16357034

70. M. Bonsignori *et al.*, Analysis of a clonal lineage of HIV-1 envelope V2/V3 conformational epitope-specific broadly neutralizing antibodies and their inferred unmutated common ancestors. *J. Virol.* **85**, 9998–10009 (2011). doi: 10.1128/JVI.05045-11; pmid: 21795340

71. H. X. Liao *et al.*, Co-evolution of a broadly neutralizing HIV-1 antibody and founder virus. *Nature* **496**, 469–476 (2013). doi: 10.1038/nature12053; pmid: 23552890

72. T. B. Kepler *et al.*, Reconstructing a B-cell clonal lineage. II. Mutation, selection, and affinity maturation. *Front. Immunol.* **5**, 170 (2014). doi: 10.3389/fimmu.2014.00170; pmid: 24795717

SUPPLEMENTARY MATERIALS

Diversion of HIV-1 vaccine–induced immunity by gp41-microbiota cross-reactive antibodies
Wilton B. Williams *et al.*
Science **349**, (2015);
DOI: 10.1126/science.aab1253